JOURNAL OF Materials CHEMISTRY

Kinetics of the cubic to trigonal transformation in $ZrMo_2O_8$ and their dependence on precursor chemistry

Cora Lind,[a] Angus P. Wilkinson,[a] Claudia J. Rawn[b] and E. Andrew Payzant[b]

[a]*School of Chemistry & Biochemistry, Georgia Institute of Technology, Atlanta, GA 30332-0400, USA. E-mail: angus.wilkinson@chemistry.gatech.edu*
[b]*Metals and Ceramics Division, Oak Ridge National Laboratory, Oak Ridge, TN 37831-6064, USA*

Received 12th September 2001, Accepted 12th November 2001
First published as an Advance Article on the web 21st February 2002

The negative thermal expansion material cubic $ZrMo_2O_8$ is metastable with respect to other polymorphs at all temperatures. On heating to temperatures >390 °C it readily transforms to trigonal $ZrMo_2O_8$. The kinetics of this transformation have been studied by *in situ* XRD and were found to be strongly influenced by the precursor chemistry used to prepare the cubic material. The conversion can be described with an Avrami model. An Arrhenius analysis of the estimated rate constants for two samples gave apparent activation energies of 269 and 291 kJ mol^{-1}. Extrapolation of the kinetic data to lower temperatures than those used for the measurements indicates that cubic $ZrMo_2O_8$ can be used for many years at temperatures below 280 °C without significant transformation.

Introduction

Negative thermal expansion (NTE) materials have received considerable attention during the last decade,[1–4] as they are of interest for use in composites and as substrates to counterbalance the positive thermal expansion of other materials. One of the most promising families of NTE materials is that with the cubic AM_2O_8 structure, where A can be Zr or Hf and M can be Mo or W. All of these compounds show isotropic NTE over a large temperature range (0.3–1050 K for ZrW_2O_8[5] and 11–573 K for $ZrMo_2O_8$[6]). The parent compound cubic ZrW_2O_8 is thermodynamically stable at high temperatures (1105–1257 °C)[7] and metastable with respect to the binary oxides below ~775 °C. It undergoes a temperature induced order–disorder phase transition from the cubic α- to the cubic β-phase at ~155 °C, which changes the relative linear expansion coefficient from -8.8×10^{-6} K^{-1} to -4.9×10^{-6} K^{-1}.[5] Its use in some composites is limited by the occurrence of a phase transformation to an orthorhombic structure at 0.21 GPa, which is not reversible at ambient temperature.[8–10] However, HfW_2O_8 displays superior characteristics at high pressure. It transforms to the orthorhombic structure at 0.62 GPa.[11]

We have previously described the synthesis of the NTE material cubic $ZrMo_2O_8$ by dehydration of $ZrMo_2O_7(OH)_2 \cdot 2H_2O$.[6,12] Unlike ZrW_2O_8, $ZrMo_2O_8$ undergoes a reversible phase transition between 0.7 and 2.0 GPa under hydrostatic conditions.[13] Cubic $ZrMo_2O_8$ is metastable with respect to the previously known monoclinic and trigonal polymorphs at all temperatures and readily converts to the trigonal form on heating to a sufficiently high temperature (>390 °C). Prior to the use of cubic $ZrMo_2O_8$ in controlled thermal expansion composites, the cubic to trigonal conversion needs to be examined in detail, so that the composite's useful lifetime at a specified temperature can be estimated.

Several kinetic models have been used to describe solid–solid transformations. Examples include diffusion-limited growth (diffusion model), nucleation on the surfaces of particles and growth towards the center (contracting volume and contracting area models), nucleation obeying a power law with constant reaction interface advance (power law model) or random nucleation with normal growth terminated by impingement of nuclei (Avrami model).[14] The Avrami model[15–17] has been widely used to describe crystalline-to-crystalline phase transformations and the crystallization of amorphous materials, for example transformations in glasses,[18,19] gels,[20,21] steels and metal alloys,[22–24] polymers,[25] and inorganic oxide materials.[26] It makes the following assumptions:[27] (i) the system is of infinite size (boundary effects can be ignored), (ii) nucleation is an independent uniform and random process and (iii) the particles grow continuously until the growth is terminated by impingement on other growing nuclei. Any solid-state transformation A → B following Avrami behavior can be described by the following equations:

$$X_B(t) = 1 - \exp\{-(k_B t)^{n_B}\} \text{ (phase B)} \quad (1a)$$

$$X_A(t) = \exp\{-(k_A t)^{n_A}\} \text{ (phase A)} \quad (1b)$$

where $X(t)$ is the mole fraction at time t, k the rate constant and n the reaction order. These equations can be converted to the linearized forms

$$\ln[-\ln\{1 - X_B(t)\}] = n_B \ln(k_B) + n_B \ln(t) \text{ (phase B)} \quad (2a)$$

$$\ln[-\ln\{X_A(t)\}] = n_A \ln(k_A) + n_A \ln(t) \text{ (phase A)} \quad (2b)$$

The $X(t)$ data needed to study solid-state transformations can be obtained in several different ways including thermal analysis[28] and *in situ* diffraction measurements.[29–33] Isothermal experiments at several different temperatures allow the determination of phase fractions as a function of time at each temperature. This information can be used to extract rate constants and activation energies from the data.

In this paper, we present an *in situ* isothermal time-resolved X-ray diffraction study of the cubic to trigonal transformation for $ZrMo_2O_8$. Two samples that displayed *ex situ* transformation behavior that was representative of most high quality cubic $ZrMo_2O_8$ batches[12] were examined. These samples were prepared using different precursor chemistry.

 DOI: 10.1039/b108350n

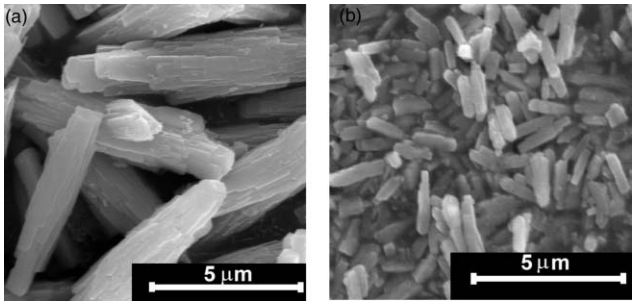

Fig. 1 SEM pictures of the cubic $ZrMo_2O_8$ samples a) C (chloride route) and b) PC (perchlorate route).

Experimental

Materials

Cubic $ZrMo_2O_8$ was synthesized by the careful dehydration of $ZrMo_2O_7(OH)_2{\cdot}2H_2O$ as described elsewhere.[6,12] Two cubic $ZrMo_2O_8$ batches were studied. One was prepared from $ZrOCl_2$, $(NH_4)_6Mo_7O_{24}$ and HCl, and the other was prepared from $ZrO(ClO_4)_2$, $(NH_4)_6Mo_7O_{24}{\cdot}4H_2O$ and $HClO_4$. They will be subsequently referred to as samples C (chloride route) and PC (perchlorate route) respectively (in a previous publication[12] they were labeled as samples CLA9 and CLA74, respectively). *Ex situ* heating and diffraction measurements suggested that samples C and PC were representative of most high quality cubic $ZrMo_2O_8$ samples that we have prepared.[12] The only crystalline phase in the samples was cubic $ZrMo_2O_8$. However, sample C contained an amorphous component ($\sim$8 weight%).[12]

SEM measurements

The size and shape of the particles in the cubic $ZrMo_2O_8$ samples were examined with a Hitachi S800 FEG scanning electron microscope (Fig. 1) operating with a 15 kV accelerating voltage.

Time resolved X-ray diffraction measurements

X-Ray diffraction experiments were carried out in air on a Scintag PAD X diffractometer with a goniometer radius of 220 mm, a sealed copper tube and an mBraun linear position sensitive detector (PSD)[34] covering a 10° range centered at 24° 2θ. A Bühler HDK2.3 accessory equipped with a Pt20%Rh heater strip and a type S thermocouple was used to heat the samples.[35] The tube was run at 10 mA and 45 kV to keep the detector well within its linear range. The thermocouple calibration was checked by optical pyrometry.

In a typical experiment, the sample was ground and suspended in methanol. The suspension was dripped on the heater strip, where the methanol was allowed to evaporate. To obtain a reproducible irradiated volume, any material located outside an area of 10 mm length around the center of the strip heater was removed.

Diffraction data were acquired as follows. For each specimen, a pattern was collected at room temperature. It was then heated rapidly to the target temperature (between 410 and 510 °C), equilibrated for 30 seconds, and between 50 and 270 consecutive patterns were collected at each temperature. Acquisition times ranged from 6 seconds ($T \geqslant 500$ °C) to 300 seconds ($T = 410$ °C). At the end of each run, the sample was heated to 700 °C for one minute to ensure complete conversion, and one to five patterns of the trigonal material were acquired after cooling back to each run temperature. Data from a typical run can be seen in Fig. 2.

The following data sets were acquired: sample C, 7 runs between 410 and 500 °C; sample PC, 7 runs between 410 and 510 °C (see Tables 1 and 2 for the temperatures that were used).

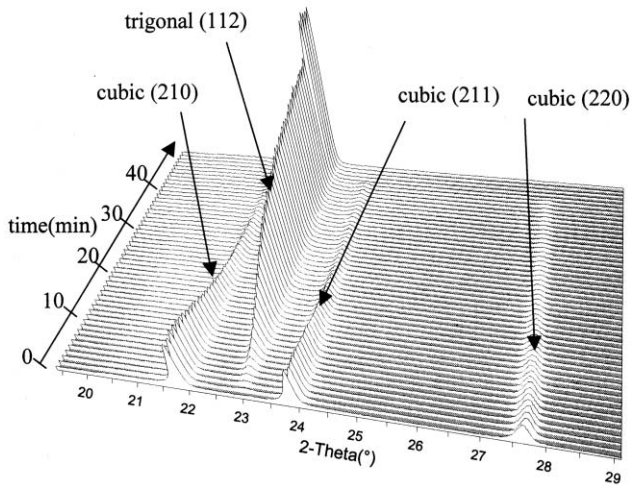

Fig. 2 Diffraction data collected for cubic $ZrMo_2O_8$ (sample C) while heating at 450 °C. A data acquisition time of one minute per pattern was used. The last five scans were collected after heating to 700 °C and cooling back to 450 °C.

Table 1 Estimated rate constants [ln (k)] and reaction orders [n] for the conversion of cubic to trigonal $ZrMo_2O_8$ (sample C). Values were obtained by the analysis of the $X(t)$ curves for both the cubic and trigonal phases.

T/°C	n [cubic]	n [trigonal]	ln (k) [cubic]	ln (k) [trigonal]
410	1.99	1.98	−6.33	−6.41
430	1.70	1.45	−4.70	−4.86
450	1.63	1.39	−3.06	−3.19
460	1.46	1.38	−3.01	−3.08
470	1.31	1.46	−2.43	−2.53
480	1.56	1.50	[a]	[a]
500	1.63	1.66	−0.70	−0.78

[a]Conversion did not proceed to a sufficient extent during the measurement period for the estimation of a rate constant by the $t_{0.37}$ method.

Table 2 Estimated rate constants [ln (k)] and reaction orders [n] for the conversion of cubic to trigonal $ZrMo_2O_8$ (sample PC). Values were obtained by the analysis of the $X(t)$ curves for both the cubic and trigonal phases

T/°C	n [cubic]	n [trigonal]	ln (k) [cubic]	ln (k) [trigonal]
410	1.18	1.26	−8.22	−8.33
440	1.85	1.81	−5.29	−5.38
460	1.84	1.69	[a]	[a]
480	2.10	1.97	−3.34	−3.38
490	2.03	1.83	−2.35	−2.43
500	2.14	1.91	−1.92	−2.04
510	2.06	2.11	−1.60	−1.68

[a]Conversion did not proceed to a sufficient extent during the measurement period for the estimation of a rate constant by the $t_{0.37}$ method.

Data analysis

Peak areas for the cubic (210) and (211) peaks and the trigonal (112) peak were estimated from the diffraction data using the program JADE.[36] The values were normalized assuming that the mole fraction of the cubic material was 1 at $t = 0$, and that for the trigonal material was 1 after heating to 700 °C. The mole fractions as a function of time are shown in Fig. 3 for sample PC. The program Isokin[37] was used to compare the data to 17 different kinetic models. The most appropriate model, as indicated by Isokin, was then used in a quantitative analysis. An Avrami model was found to be appropriate. The

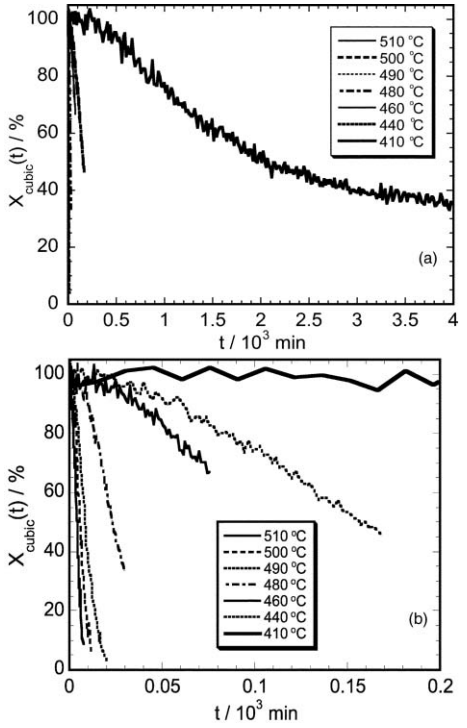

Fig. 3 Mole fractions of the cubic phase as a function of time and temperature for sample PC (perchlorate route). b) shows an expanded version of the short time region in graph a).

data for samples C and PC were further analyzed using a linearized version of the Avrami equation (Fig. 4).

Rate constants were extracted using the "$t_{0.37}$ method". $t_{0.37}$ is defined as the time when $X(t) = 0.37 = e^{-1}$ for the transforming phase. At this time, $kt = 1$ and thus $k = t^{-1}$ independent of n. For the growing phase, $X(t_{0.63})$ can be used. For each sample, one run had to be excluded from the analysis, as the conversion had not proceeded far enough to estimate $t_{0.37}$. The exponent, n, was determined by fitting the data to eqn. (2a) or (2b). No constraint on the value of k was employed when estimating n. The ln (k) values resulting from linear regression were similar to those extracted by the $t_{0.37}$ method.

It is important to recognize that the data range used in the fitting can influence the extracted values for the slope and intercept. Many solid–solid phase transitions show an induction period. Also, some materials do not exhibit complete conversion at low temperatures, instead, the conversion levels off at a certain percentage. This results in curvature of the linearized plots. In the cases where this was a problem, the data were cut at low and high conversion times and only the linear region was fitted. This limits the accuracy of the extracted rate constants and reaction orders, and can lead to errors in the estimated lifetimes.

The rate constants (see Tables 1 and 2) were used to estimate the activation energy for the cubic to trigonal transformation using the Arrhenius equation:

$$k = A\exp(-E_a/RT) \quad (3)$$

where k is the rate constant, A a preexponential or "frequency" factor, E_a the activation energy, R the gas constant and T the temperature in Kelvin. The estimated values for E_a and A are given in Table 3.

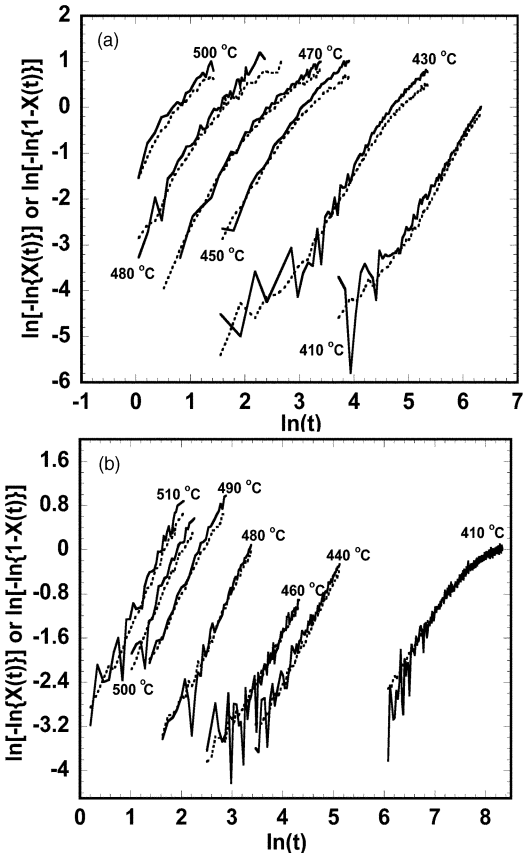

Fig. 4 Avrami plots for the conversion of samples a) C (chloride route) and b) PC (perchlorate route) at different temperatures. The solid lines are for the cubic phase and the dotted lines represent the trigonal phase.

Results and discussion

The kinetics of the cubic to trigonal conversion were very different for the two studied samples. The conversion rates followed the trend sample PC < sample C. For sample C, the curves for $X_{cubic}(t)$ and $X_{trigonal}(t)$ generally intersected at $X(t) \sim 0.45$. For most runs, $X_{cubic}(t) + X_{trigonal}(t)$ showed a deviation from 1.0 to lower values at intermediate times.

The program Isokin indicated that all the data could be fitted with an Avrami model. It should be noted that the conversion did not go to completion at low temperatures (see Fig. 3 a).

Rietveld quantitative phase analyses indicated that sample PC was 100% crystalline, while sample C contained ~8% amorphous material. This should lead to identical Avrami plots for the cubic and trigonal phases in sample PC. However, the lines would be expected to deviate from each other for sample C. This is confirmed by the data in Fig. 4. For sample C, the line for the trigonal phase has a lower value than that of the cubic phase at nearly all temperatures. This is consistent with the presence of an amorphous phase that is converted to trigonal material more slowly than the cubic phase or only at higher temperatures (*e.g.* while heating to 700 °C). Normalization to the 100% trigonal peaks after heating to 700 °C would then result in systematically lower values for the amount of trigonal phase than expected from the amount of converted cubic phase. The effect of the amorphous phase can also be seen by examining the sum of the phase fractions $X_{cubic}(t)$ +

Table 3 Activation energies and preexponential factors from an Arrhenius analysis of the rate constants for both the formation of trigonal $ZrMo_2O_8$ and the decay of cubic $ZrMo_2O_8$ in samples C and PC

Phase	E_a/kJ mol^{-1}	A/s^{-1}
Sample C cubic	268.0	7.0E + 17
Sample C trigonal	269.9	8.5E + 17
Sample PC cubic	290.4	5.9E + 18
Sample PC trigonal	291.3	6.3E + 18

$X_{trigonal}(t)$. It is slightly less than 1 at intermediate reaction times.

All the data could be analyzed using the linearized Avrami equations [eqn. (2a) and (2b)]. While the rate constants obtained from the $X(t)$ curves for the cubic and trigonal phases in each sample agreed with each other within experimental error, the values for samples C and PC at the same temperature were quite different, indicating that the conversion kinetics depend on the method used to prepare the cubic $ZrMo_2O_8$. The reaction orders varied between 1.20 and 2.15. For many of the data sets the values obtained from the $X(t)$ curves for the cubic and trigonal phases were close to one another as might be expected, but considerable deviations were observed at some temperatures. This is a consequence of the high noise level in the data used to estimate n (see for example the 460 °C run for sample PC in Fig. 4 b). After excluding the data at short times and the 100% conversion values, the lines for the cubic and trigonal phases followed the same trend, but the large noise spikes gave a smaller reaction order for the cubic phase during the linear regression. The noise spikes may arise from uncertainties in the background fitting. Our estimate of the peak areas for the cubic phase were more prone to errors of this type than those for the trigonal phase.

The 410 °C data for sample PC demonstrated the curvature that can arise from incomplete conversion and leveling off of $X(t)$ values at long times. Temperature dependent conversion levels have been previously observed for other solid–solid transformations.[38–41] Magee[40] explained this phenomenon for polycrystalline or powdered samples by pointing out that the defects and imperfections acting as nucleation sites can show a distribution of activation energies between E_a^{min} and E_a^{max}. For samples with large grains, the probability is high that all grains contain at least one defect with the minimum activation energy E_a^{min}. With decreasing grain size, however, the probability increases that a fraction of the grains will have only defects with higher activation energies than E_a^{min}. These grains will only transform at temperatures that are sufficient to overcome this barrier, while grains with E_a^{min} will transform at lower temperatures. This results in an increase of the extent of sample conversion with temperature. The conversion of sample C leveled off at ~90–95% for temperatures below 470 °C. Complete conversion was observed at higher temperatures. While the leveling off could indicate that the ~8% amorphous phase only converted at higher temperatures, the presence of small cubic peaks suggested that this was due to the incomplete conversion of the cubic phase. For sample PC, which had smaller particles than sample C (see Fig. 1), complete conversion was observed at 500 and 510 °C, and at 490 °C complete conversion might have occurred at longer times. The 410 °C data leveled off at about 60–65% conversion, and the 420 °C data (not used for quantitative analysis due to peak shape problems) showed about 70–80% conversion at the end of the run. The runs collected between 440 and 480 °C might level off, but the total experiment times were too short to draw a reliable conclusion. These observations are consistent with Magee's ideas. For sample PC, renormalization of the 410 °C run by assuming that $X_{trigonal} = 1$ when the maximum extent of conversion was reached gave a reaction order of 1.55 (without renormalization: 1.26) and an ln (k) value of −7.4 (without renormalization: −8.3). The renormalization produced Avrami plots that did not display curvature at long times. The incomplete conversion observed at low temperatures can have a significant effect on lifetime estimates, as extrapolations based on the high temperature data do not take this into account.

The rate constants were used in an Arrhenius analysis (see Fig. 5). The activation energies and preexponential factors that were estimated using the rate constants from the $X(t)$ data for the cubic and trigonal phases in each sample were in excellent agreement, but they were different for samples C and PC. The apparent activation energies extracted from the Avrami model

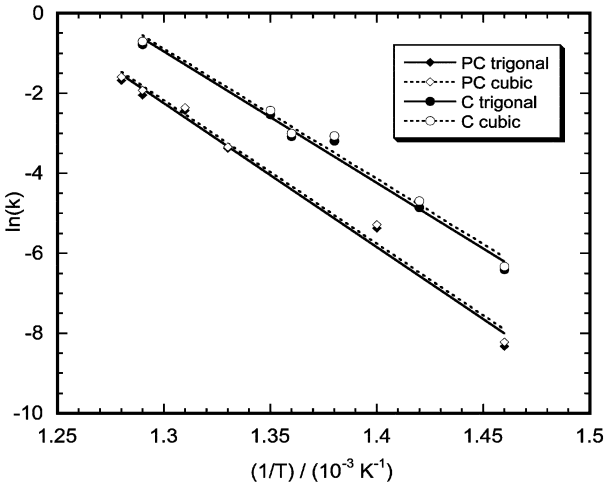

Fig. 5 Arrhenius plots for cubic $ZrMo_2O_8$ samples C (chloride route) and PC (perchlorate route).

were 269 and 291 kJ mol^{-1} for samples C and PC, respectively. This large difference may be connected with the microstructures of the samples (see Fig. 1). The material prepared using the chloride route consists of large aggregates of rods, whereas the material prepared by the perchlorate route contains smaller rod like particles.

While we successfully determined activation energies for the conversion of cubic to trigonal $ZrMo_2O_8$ at high temperature using our diffraction data, in general, the determination of accurate kinetic parameters and their extrapolation to temperatures beyond those used in their determination is not straightforward. The experimental methods, data handling procedures and theoretical modeling of the data all contribute to the uncertainties. The experimental difficulties include achieving a well-known, uniform sample temperature[35] in a short period of time and reproducibly preparing specimens that are representative of the bulk material. During data processing there can be problems associated with the correct normalization of the $X(t)$ data. Additionally, the models commonly used for analyzing the kinetic data are limited in their ability to describe complex systems (*e.g.*, distribution of particle sizes and activation energies).

Using the activation energies and preexponential factors from our Arrhenius analysis (Table 3) along with eqn. (1), we determined approximate lifetimes for cubic $ZrMo_2O_8$ at different temperatures. Assuming 5% conversion as the tolerance limit for good device performance, and a reaction order of $n = 2$ in the Avrami model, temperatures of 290 and 315 °C would give a lifetime of ~1 year for samples C and PC, respectively. These values can be considered as a lower limit, as at least for sample PC the reaction order appeared to decrease with decreasing temperature. Fig. 6 shows estimated lifetime values for both samples at various temperatures. However, if the leveling off in the data for sample PC observed at low temperatures was considered and the data renormalized as previously discussed, an activation energy of 257 kJ mol^{-1} and a preexponential factor of 2.7×10^{16} were obtained from the data for the trigonal phase of sample PC. This would lead to an estimated lifetime of one year at ~295 °C, for 5% conversion of the convertible fraction in the sample. Assuming that 10% of this fraction would have to convert to get an overall conversion of ~5%, a temperature of ~310 °C should give a one year lifetime. It seems possible that the true lifetime is longer, as the fraction of converting material may decrease with decreasing temperature. This would make lifetime predictions by extrapolation to temperatures much lower than those investigated during the experiments inaccurate. *Ex situ* experiments have shown that the conversion of sample C at 390 °C proceeds

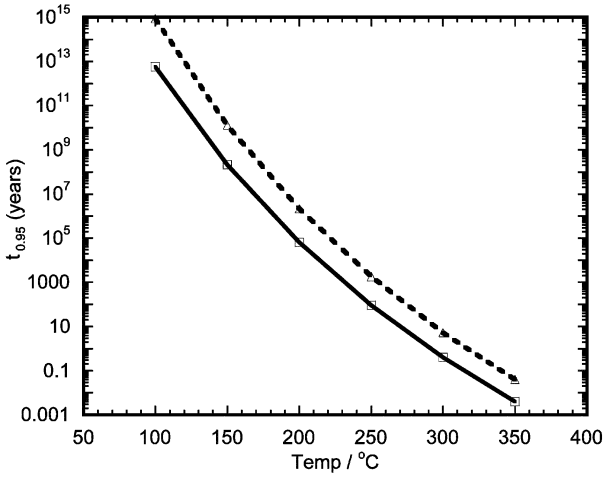

Fig. 6 The temperature dependence of the time ($t_{0.95}$) for the cubic $ZrMo_2O_8$ samples to convert into a 95% cubic–5% trigonal mixture. The times were estimated using an exponent of 2 in the Avrami equation and activation energies/preexponential factors from the Arrhenius analyses.

slower than predicted by extrapolation from our experimental data. No conversion could be detected at all after holding times that were longer than our predicted $t_{0.95}$ at 390 °C.

Conclusions

The kinetics of the cubic to trigonal transformation for $ZrMo_2O_8$ are strongly dependent on the chemistry used to prepare the cubic samples, presumably due to the different particle sizes and nucleation sites that are available. At low temperatures, the conversion of cubic to trigonal material reaches a plateau. This could result from a distribution of activation energies for the nucleation sites. An Arrhenius analysis of the rate constants provided preexponential factors and activation energies that could be used to estimate a "useful lifetime" for cubic $ZrMo_2O_8$ as a function of temperature. The time for 5% conversion changes by a factor of $\sim$10 from sample C to PC. Our data suggest that cubic $ZrMo_2O_8$ can be safely used at temperatures of up to 280 °C (5% conversion will take several years), and that it will withstand short time periods at temperatures up to 300–320 °C. This should include the working temperature range for many applications.

Acknowledgement

This research was supported by the National Science Foundation through grant DMR-9623890 and the Office of Naval Research through the Molecular Design Institute at the Georgia Institute of Technology, which is supported under ONR contract N00014-95-1-1116. Acknowledgment is made to the donors of The Petroleum Research Fund, administered by the American Chemical Society, for partial support of this research under contract number 35087-AC5. The XRD data were collected at the Diffraction User Center, Oak Ridge National Laboratory, sponsored by the Assistant Secretary for Energy Efficiency and Renewable Energy, Office of Transportation Technologies, as part of the High Temperature Materials Laboratory User Program, Oak Ridge National Laboratory, managed by UT-Battelle, LLC, for the U.S. Dept. of Energy under contract DE-AC05-00OR22725. We are grateful to the Georgia Tech Microscopy Center for providing the research facilities used in the microstructural characterization.

References

1 A. W. Sleight, *Inorg. Chem.*, 1998, **37**, 2854.
2 A. W. Sleight, *Curr. Opin. Solid State Mater. Sci.*, 1998, **3**, 128.
3 A. W. Sleight, *Ann. Rev. Mater. Sci.*, 1998, **28**, 29.
4 J. S. O. Evans, *J. Chem. Soc., Dalton Trans.*, **1999**, 3317.
5 T. A. Mary, J. S. O. Evans, T. Vogt and A. W. Sleight, *Science*, 1996, **272**, 90.
6 C. Lind, A. P. Wilkinson, Z. Hu, S. Short and J. D. Jorgensen, *Chem. Mater.*, 1998, **10**, 2335.
7 C. A. Martinek and F. A. Hummel, *J. Am. Ceram. Soc.*, 1970, **53**, 159.
8 J. S. O. Evans, Z. Hu, J. D. Jorgensen, D. N. Argyriou, S. Short and A. W. Sleight, *Science*, 1997, **275**, 61.
9 C. Verdon and D. C. Dunand, *Scr. Mater.*, 1997, **36**, 1075.
10 H. Holzer and D. C. Dunand, *J. Mater. Res.*, 1999, **14**, 780.
11 J. D. Jorgensen, Z. Hu, S. Short, A. W. Sleight and J. S. O. Evans, *J. Appl. Phys.*, 2001, **89**, 3184.
12 C. Lind, A. P. Wilkinson, C. J. Rawn and E. A. Payzant, *J. Mater. Chem.*, 2001, **11**, 3354.
13 C. Lind, D. G. VanDerveer, A. P. Wilkinson, J. Chen, M. T. Vaughan and D. J. Weidner, *Chem. Mater.*, 2001, **13**, 487.
14 C. H. Bamford and C. F. H. Tipper, *Reactions in the Solid State*, Elsevier Scientific Publishing Company, Amsterdam, New York, 1980.
15 M. Avrami, *J. Chem. Phys.*, 1939, **7**, 1103.
16 M. Avrami, *J. Chem. Phys.*, 1940, **8**, 212.
17 M. Avrami, *J. Chem. Phys.*, 1941, **9**, 177.
18 Y. M. Sung and S. Kim, *J. Mater. Sci.*, 2000, **35**, 4293.
19 A. F. Gualtieri, E. Mazzucato, C. C. Tang and R. J. Cernik, *Mater. Sci. Forum*, 2000, **312–3**, 224.
20 A. M. Fogg, S. J. Price, R. J. Francis, S. O'Brien and D. O'Hare, *J. Mater. Chem.*, 2000, **10**, 2355.
21 J. Malek, *Thermochim. Acta*, 2000, **355**, 239.
22 D. V. Louzguine and A. Inoue, *J. Mater. Sci.*, 2000, **35**, 4159.
23 J. K. Lee, G. Choi, D. H. Kim and W. T. Kim, *Appl. Phys. Lett.*, 2000, **77**, 978.
24 C. A. C. Imbert and H. J. MacQueen, *Mater. Sci. Technol.*, 2000, **16**, 532.
25 M. J. Jenkins, *Polymer*, 2001, **42**, 1981.
26 P. Norby, A. N. Christensen and J. C. Hanson, *Inorg. Chem.*, 1999, **38**, 1216.
27 M. Weinberg and R. Kapral, *J. Chem. Phys.*, 1989, **91**, 7146.
28 M. E. Brown, *J. Therm. Anal.*, 1997, **49**, 17.
29 C. Riekel, *Prog. Solid State Chem.*, 1980, **13**, 89.
30 J. Pennetier, *Chem. Scr.*, 1986, **26A**, 131.
31 M. C. Morón, *J. Mater. Chem.*, 2000, **10**, 2617.
32 A. K. Cheetham and C. F. Mellot, *Chem. Mater.*, 1997, **9**, 2269.
33 R. I. Walton and D. O'Hare, *Chem. Commun.*, 2000, 2283.
34 E. A. Payzant and W. S. Harrison, *Adv. X-Ray Anal.*, 2000, **43**, 267.
35 H. Wang and E. A. Payzant, *Proc. SPIE – Int. Soc. Opt. Eng.*, 1999, **3700**, 377.
36 JADE, a program for powder diffraction data analysis, Materials Design Inc., Livermore, CA, USA.
37 Isokin, a program for modeling solid-state isothermal kinetic data (1989). Developed and distributed by J. Anwar, Department of Pharmacy, King's College London, Manresa Road, London, UK SW3 6LX.
38 A. K. Sheridan and J. Anwar, *Chem. Mater.*, 1996, **8**, 1042.
39 R. E. Cech and D. Turnbull, *AIME Trans.*, 1956, **206**, 124.
40 C. L. Magee, *Metall. Trans.*, 1971, **2**, 2419.
41 V. Raghaven and M. Cohen, *Metall. Trans.*, 1971, **2**, 2409.